Biochemical and Biophysical Research Communications 459 (2015) 100–106

Contents lists available at ScienceDirect

Biochemical and Biophysical Research Communications

journal homepage: www.elsevier.com/locate/ybbrc

Phosphorylation of voltage-dependent anion channel by c-Jun N-terminal Kinase-3 leads to closure of the channel

Rajeev Gupta, Subhendu Ghosh*

Department of Biophysics, University of Delhi South Campus, New Delhi, India

ARTICLE INFO

Article history:
Received 2 February 2015
Available online 23 February 2015

Keywords:
VDAC
Bilayer electrophysiology
Phosphorylation
JNK3
Mitochondria-mediated apoptosis

ABSTRACT

Stress activated c-Jun N-terminal Kinase-3 (JNK3) has been reported to act on mitochondrion to promote neuronal cell death. Phosphorylation of mitochondrial Voltage-Dependent Anion Channel (VDAC) plays an important role in mitochondria-mediated cell death. Keeping these in view phosphorylation of rat brain VDAC by JNK3 has been studied *in vitro*. Pro Q Diamond phospho-protein staining experiment demonstrates VDAC is phosphorylated by JNK3. Bilayer electrophysiological experiments show that single-channel conductance of VDAC phosphorylated by JNK3 is significantly lower than that of the native VDAC at a membrane potential. The opening probability of VDAC undergoes massive reduction due to phosphorylation by JNK3. These indicate closure of VDAC due to phosphorylation by JNK3. Treatment of phosphorylated VDAC with alkaline phosphatase reversed the VDAC functional activity as shown by single-channel current and opening probability. The physiological consequence of closure of VDAC as a result of phosphorylation has been attributed to JNK3 dependent mitochondria-mediated apoptosis.

© 2015 Elsevier Inc. All rights reserved.

1. Introduction

Post-translational modifications like phosphorylation, nitration, acetylation and palmitoylation etc. of membrane proteins have been known to be important in a number of biological processes [1,2]. Especially ion channel proteins have been reported to be functionally regulated by biochemical modifications like phosphorylation [3]. At the outer mitochondrial membrane Voltage-Dependent Anion Channel (VDAC) controls the flux of ions, water and essential metabolites between the cytosol and the mitochondrion by gating or opening-closing [4]. There are three isoforms of VDAC and all three have been shown to undergo post-translational modifications in biological systems [5,6]. VDAC phosphorylation has been reported in many disorders like fatty liver disease, ischemia-reperfusion injury and in cancer metabolism [7,8,15]. Different cytosolic protein kinases, such as Protein Kinase A, Protein Kinase B (Akt), Protein Kinase C, Tyrosine Protein Kinase, Hexokinase, Glycogen Synthase Kinase-3β (GSK3β), Nek1 kinase also known as NIMA Kinase (never-in- mitosis A related Kinase-1) and p38 MAPK (Mitogen Activated serine–threonine Protein Kinase) regulate outer mitochondrial membrane permeability by phosphorylating VDAC [9,10]. Phosphorylation of VDAC by Protein Kinase A has been reported to partially close down the channel [11,12]. The gating properties of VDAC and its role in cytochrome *c* mediated apoptosis have been extensively studied by various groups [13–16].

c-Jun N-terminal Kinases (JNKs) are cytosolic Stress/Mitogen Activated serine–threonine Protein Kinases (SAPKs/MAPKs). JNKs have been linked to numerous physiological and pathological processes including neuronal cell death leading to neurodegenerative disorders like Alzheimer's disease, Parkinson's disease etc. by the mitochondria-mediated pathway [17]. There are ten isoforms of JNKs, all of those are found in human adult brain with JNK3 being the principal neuron specific isoform. They are activated by dual phosphorylation on their Threonine (Thr) and Tyrosine (Tyr) residues in the Thr-Pro-Tyr motif by upstream kinases [18]. Activated JNKs phosphorylate Ser/Thr–Pro motifs in target proteins [18]. During stress activated JNKs translocate to mitochondria and phosphorylate mitochondrial outer membrane associated proteins [19,20]. It has been reported that arsenic oxide induces mitochondria-mediated apoptosis in cervical cancer cells by the activation of JNK pathway and dimerization of VDAC [16]. Ischemia/

Abbreviations: BLM, bilayer lipid membrane; VDAC, voltage-dependent anion channel; kDa, kiloDaltons; JNK3, c-Jun N-terminal Kinase-3; PhosphoVDAC, phosphorylated VDAC; tBid, truncated Bid.

* Corresponding author. Fax: +91 11 24115270.
E-mail address: profsubhendu@gmail.com (S. Ghosh).

http://dx.doi.org/10.1016/j.bbrc.2015.02.077
0006-291X/© 2015 Elsevier Inc. All rights reserved.

Reperfusion injury in kidney leads to apoptosis with increased levels of caspase 12, cytochrome *c*, phosphorylated JNK and phosphorylated VDAC [21]. As per our knowledge there are no direct reports on VDAC phosphorylation by JNK3. As mentioned earlier VDAC phosphorylation plays an important role in many disorders. Here we hypothesize that JNK3 phosphorylates brain mitochondrial VDAC, thus regulates its gating properties. In the present work we have studied the phosphorylation of VDAC by JNK3 using phospho-protein staining and bilayer electrophysiological experiments towards establishing our hypothesis.

2. Materials and methods

2.1. Purification of VDAC

VDAC was purified in the micelles form from rat brain mitochondria using 3% Triton X-100 detergent by a standard method [22]. Permission for this animal experiment was obtained from the Committee for the Purpose of Control and Supervision of Experiments on Animals (CPCSEA), India.

2.2. Detection of VDAC phosphorylation by JNK3 using Pro Q diamond staining method

Purified VDAC (approximately 12 ml) was treated with washed SM-2 Bio-Beads (Bio-Rad Laboratories, CA, USA) to remove the unbound Triton X-100 so as to prevent detergent interference on Pro Q Diamond dye binding (Pro Q Diamond dye binds to the phosphate groups nonspecifically and thus identifies phosphorylated proteins distinctly from the unphosphorylated ones). As we get low yield of VDAC from brain samples, VDAC was concentrated using Amicon Ultra Centrifugation filter, 10 kDa (Millipore Corp., MA, USA) to approximately 600 μl. Then, it was divided equally into three eppendorf tubes corresponding to Negative Control (VDAC + Mg^{2+}ATP), Experimental Sample (VDAC + JNK3 + Mg^{2+}ATP) and Positive Control [VDAC + JNK3 + Mg^{2+}ATP + Alkaline Phosphatase (added later)]. 0.32 μl (0.5 μg) dually phosphorylated, human, recombinant, His-JNK3 enzyme having more than 200 units/mg activity (Enzo LifeSciences, USA), ATP (Final concentration 100 μM) and $MgCl_2$ (Final concentration 10 mM) were added to the respective tubes. Phosphorylation reaction was carried out by incubating the cocktail at 30 °C for 30 min. In the Positive Control, 0.5 μl (0.1 mg) of calf intestinal alkaline phosphatase prepared in 10 mM HEPES-KOH buffer (pH 7.4) was added and incubated for another 30 min at 30 °C. The samples were precipitated using chloroform: methanol mixture. Protein pellets were air dried and dissolved in 1X sample buffer. All the tubes were boiled for 5 min at 100 °C along with the peppermint stick phosphoprotein molecular weight standards (Molecular probes, Inc., Eugene, OR, USA), 2 μl in 12 μl of 1X sample buffer. Samples were resolved on 12.5% SDS-PAGE at constant voltage (100 V) and the gel was fixed in 50% Methanol and 10% Acetic acid for 30 min on a shaker. Fixative was replaced with fresh one and left overnight. Next day, gel was washed thrice with Milli-Q water for 15 min each. It was stained using Fluorescent Pro Q Diamond phosphoprotein gel stain (Molecular probes, Inc., Eugene, OR, USA) for 2 h and then destained with Pro Q Diamond phosphoprotein destaining solution (Molecular probes, Inc., Eugene, OR, USA) for 1.5 h thrice for 30 min each time in a dark room on the shaker. The gel was washed thrice for 5 min each with Milli-Q water and visualized on FLA-9000 phosphoimager (Fuji Fim Inc., Tokyo, Japan). After visualization, the gel was Silver stained to show VDAC was loaded equally in the positive and negative controls as well as in the experimental sample.

2.3. Reconstitution of VDAC on BLM

VDAC was reconstituted onto planar phospholipid bilayers as standardized in our laboratory [12,13]. Briefly, the apparatus consisted of a Perfusion BLM Cup made up of polystyrene (Warner Instruments Corp., Hamden, CT, USA) with a thin wall separating two aqueous compartments (cis and trans) of BLM chamber containing BLM buffer [1 M KCl, 10 mM $MgCl_2$, 10 mM HEPES (pH 7.4)]. The BLM Cup had a circular aperture with a diameter of 150 μm. Aqueous compartments were connected to an integrating patch clamp amplifier (Axopatch 200B, Axon Instruments, Sunnyvale, CA, USA) through a matched pair of Ag/AgCl electrodes. The cis compartment was connected to the headstage (CV203BU) of the amplifier and the trans compartment was held at virtual ground. Lipid mixture containing DPhPE (1,2-DiPhytanoyl-*sn*-glycero-3-PhosphoEthanolamine) and DPhPC (1,2-DiPhytanoyl-*sn*-glycero-3-PhosphatidylCholine) (Avanti Polar Lipids, Alabaster, AL, USA) (8:2 v/v ratio) in *n*-decane was freshly prepared such that the final lipid concentration is l2.5 mg/ml. BLM was painted by applying lipid mixture to the BLM cup aperture using a fire polished glass capillary. After formation of the BLM, 2 μl of purified rat brain VDAC solution (containing approximately 3–5 ng protein) was added to the cis chamber and the solution was slowly stirred to promote channel insertion onto BLM at + 10 mV applied potential. After insertion of the first channel, buffer in the cis chamber was perfused with fresh one devoid of VDAC using two peristaltic pumps at the flow rate of 10 ml/min. Single-Channel currents were filtered using an external low pass RC filter (Single pole) at 200 Hz and then acquired and digitized at 1 kHz Sampling frequency using data acquisition software Clampex (pClamp 10.2, Axon Instruments, Sunnyvale, CA, USA) through an analog to digital converter (Digidata 1440A, Axon Instruments, Sunnyvale, CA, USA).

2.4. Phosphorylation of VDAC on BLM

Single-channel currents were recorded through VDAC at different clamping potentials in the range of ±50 mV. After recording VDAC current at different membrane potentials the following additions were made to both the sides of the bilayer chamber: (i) 1 μl Mg^{2+}ATP (Final concentration 50 μM); (ii) 0.32 μl JNK3 (Final concentration 0.5 μg/ml); (iii) 1 μl Mg^{2+}ATP (Final concentration 50 μM) and 0.32 μl JNK3 (Final concentration 0.5 μg/ml) at room temperature. In each case, single-channel currents were once again recorded at different clamping potentials in the range of ±50 mV. Also, in case (iii) after recording currents, alkaline phosphatase (1–2 units) was added to both sides of the bilayer chamber and currents were once again recorded.

2.5. Analysis of bilayer electrophysiological data

(i). Current was obtained from the single-channel current-time traces and the current-amplitude histograms at different voltages. Finally, a comparison of the mean of the current values of three independent sets of experiments of native and on BLM phosphorylated VDAC was made by the I–V plot. I–V plot was obtained using pClamp 10.2 (Axon Instruments, Sunnyvale, CA, USA) and Origin 5.0 (Origin Lab Corp., MA, USA) software. Best fit plots of the experimental data were drawn using Origin 5.0. Histogram analysis was done using pClamp 10.2 and AxoGraph X (Version 1.5.4, AxoGraph Inc., CA, USA).

(ii). The opening probability at a particular voltage was determined by calculating the fraction of total time it remained fully open at that voltage out of total time of recording at that

particular voltage. It was calculated using pClamp 10.2 software and plotted using Origin 5.0.

3. Results

Fig. 1A shows the image of the Pro Q Diamond stained gel and Fig. 1B shows the Silver stained image of the same gel. Lane 1: Peppermintstick Phosphoprotein molecular weight standard. It contains a combination of six proteins, two are in the phosphorylated form (23.6 kDa, 45 kDa) and the rest four are in the unphosphorylated form (14.4 kDa, 18 kDa, 66.2 kDa, 116.25 kDa). Pro Q diamond dye binding was observed for only two phosphorylated proteins with molecular weight 23.6 kDa and 43 kDa in the standard sample, which authenticates the activity of the dye. Lane 2: Negative Control, i.e. VDAC (35 kDa) + Mg^{2+}ATP. We did not detect any dye binding to VDAC in this lane which confirms that VDAC is neither pre-phosphorylated nor it undergoes self-phosphorylation in the presence of ATP without the enzyme. Lane 3: JNK3 (52 kDa) enzyme. It was loaded to confirm that it is in phosphorylated form, which is the active state of the enzyme. Dye binding to the JNK3 band confirmed the same. Lane 4: Experimental Sample, i.e. VDAC + JNK3 enzyme + Mg^{2+}ATP, dye binding was observed in the VDAC band which suggests VDAC is phosphorylated by JNK3. Lane 5: Positive Control, i.e. VDAC + JNK3 enzyme + Mg^{2+}ATP + Alkaline Phosphatase. A decrease in the amount of bound dye or no dye binding in this lane after alkaline phosphatase treatment shows VDAC phosphorylation by JNK3 is reversible. As demonstrated by our repeated sets of Pro Q Diamond Staining Experiment (Fig. 1A) rat brain VDAC is phosphorylated by JNK3. In Fig. 1B equal intensity of the VDAC monomer band in the positive and negative controls as well as in the experimental sample confirms equal loading of VDAC in these lanes.

Fig. 2(A, B, C, D, E and F) shows single-channel current-time traces and their current amplitude histograms (representative) of native (unphosphorylated), phosphorylated and phosphorylated VDAC after alkaline phosphatase treatment at ± 40 mV. The single-channel current traces of native VDAC showed different sub-states as reported earlier [4,11]. However, in our analysis we have considered the full open state only. It was observed that phosphorylation of VDAC by JNK3 leads to significant closure of the channel (Fig. 2C and D) at all the voltages in the range of ±50 mV. We did not observe channel closure at any voltage when only ATP or only JNK3 was used. Fig. 3 shows the current vs. applied membrane potential (I–V) of native VDAC and phosphorylated VDAC. The figure indicates that single-channel current (full open state) of phosphorylated VDAC is significantly lower than that of native VDAC at both positive and negative clamping membrane potentials. The I–V plot for native VDAC is sigmoidal whereas that for the JNK3 phosphorylated VDAC fits a third order polynomial function, both being symmetric at positive and negative membrane potentials. Fig. 4 shows the opening probability vs. membrane potential of VDAC (native and phosphorylated). It is clear from Fig. 4 that opening probability of VDAC is drastically lowered at both positive and negative potentials due to phosphorylation by JNK3. When phosphorylated VDAC was dephosphorylated with alkaline phosphatase, we found the opening probability and single-channel current of the channel are reversed to those of native VDAC at both positive and negative membrane potentials showing the reversibility of the phosphorylation reaction. However, after dephosphorylation, the sub-states were less distinctly observed as compared to native VDAC, which is evident from the current amplitude histograms (Fig. 2E and F).

4. Discussion

As evident from Fig. 1, JNK3 phosphorylates rat brain mitochondrial VDAC *in vitro*. Our results show phosphorylation leads to decrease in single-channel current (Figs. 2 and 3) and open probability (Fig. 4) at all the membrane potentials (±50 mV). These results suggest significant closure of the channel upon phosphorylation by JNK3 at both positive and negative clamping potentials.

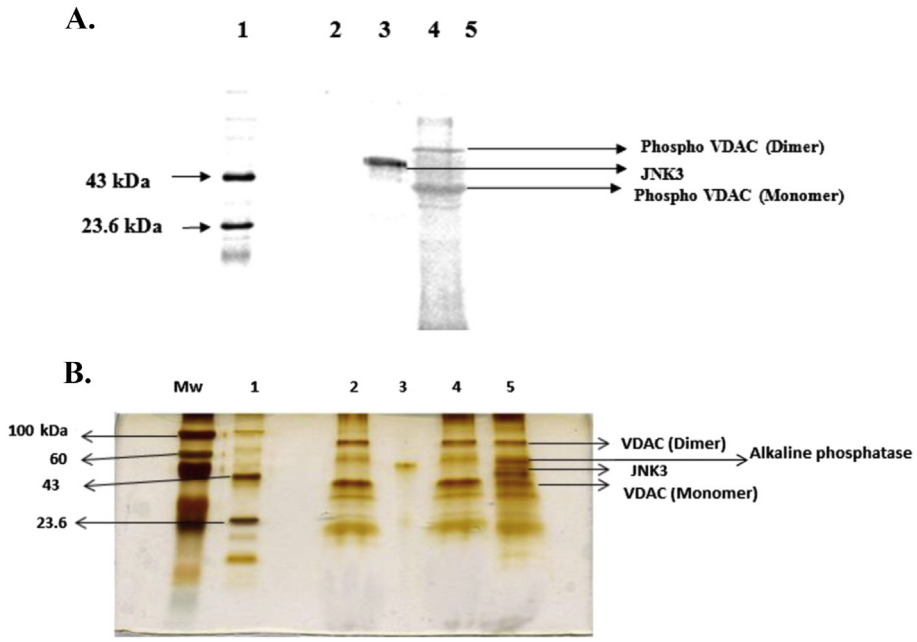

Fig. 1. A. Representative Pro Q Diamond stained SDS PAGE gel image showing phosphorylation of rat brain mitochondrial VDAC by JNK3. **Lane 1**: Phosphoprotein standard. **Lane 2**: Negative Control, i.e. VDAC + Mg^{2+}ATP. **Lane 3**: JNK3 enzyme. **Lane 4**: Experimental Sample i.e. VDAC + JNK3 + Mg^{2+}ATP. **Lane 5**: Positive Control i.e. VDAC + JNK3 + Mg^{2+}ATP + Alkaline Phosphatase. **B**. Gel image after Silver staining. **Mw**: Color Burst electrophoresis Marker C1992 (Mol wt. 8000–220,000 Da, Sigma Chem. Company, USA). The size of the gel increases when stained with Pro Q Diamond dye and decreases to the original size during Silver staining.

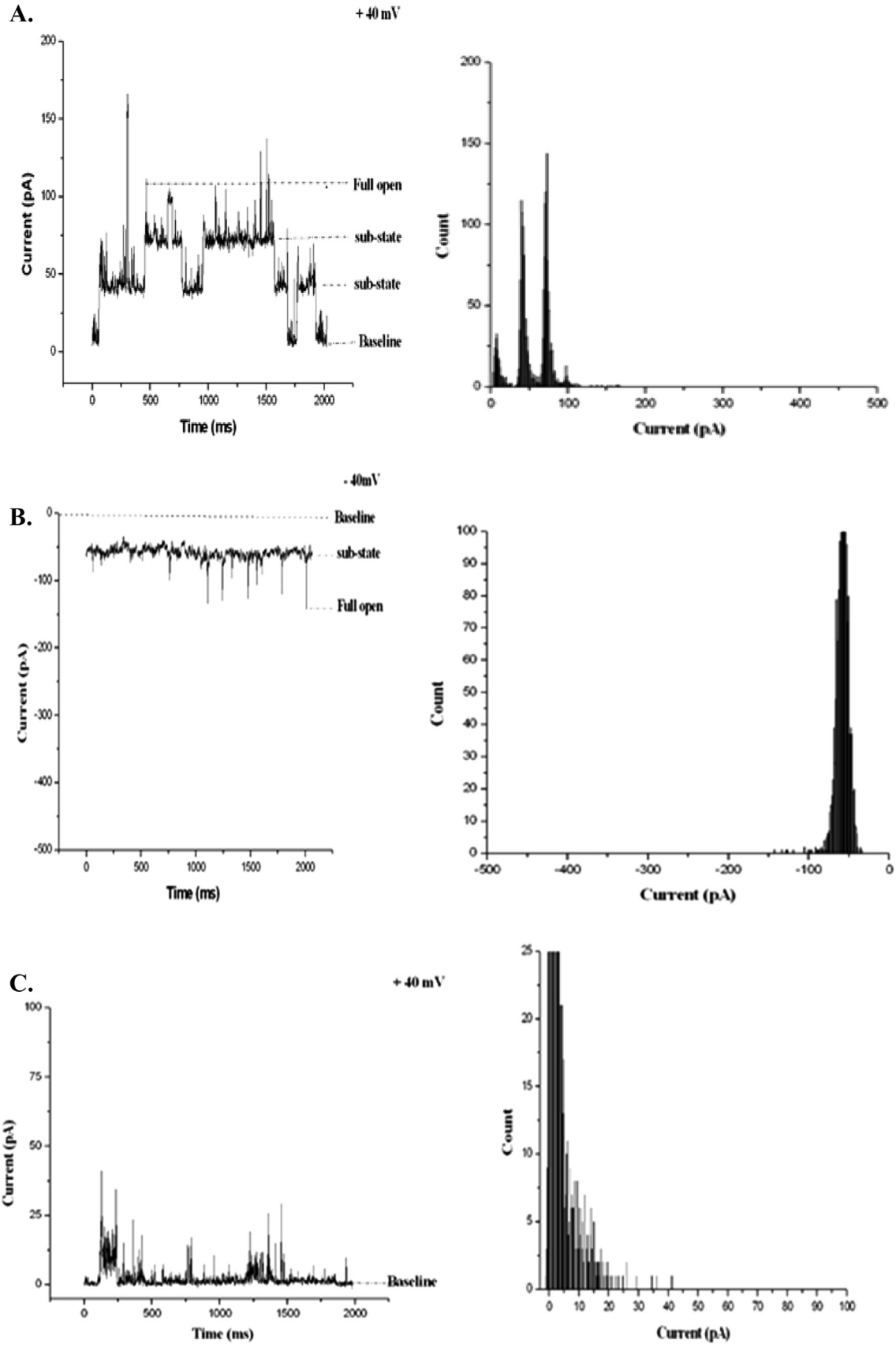

Fig. 2. Representative Single-Channel current traces and their Current Amplitude histograms of Rat brain mitochondrial VDAC on a DPhPE/DPhPC membrane (BLM) with a symmetrical bath solution of 1 M KCl, 10 mM $MgCl_2$, 10 mM HEPES, pH 7.4 at 25 °C. **A**. Native VDAC at +40 mV; **B**. Native VDAC at − 40 mV; **C**. Phosphorylated VDAC at +40 mV; **D**. Phosphorylated VDAC at − 40 mV; **E**. Phosphorylated VDAC after alkaline phosphatase treatment at +40 mV; **F**. Phosphorylated VDAC after alkaline phosphatase treatment at − 40 mV.

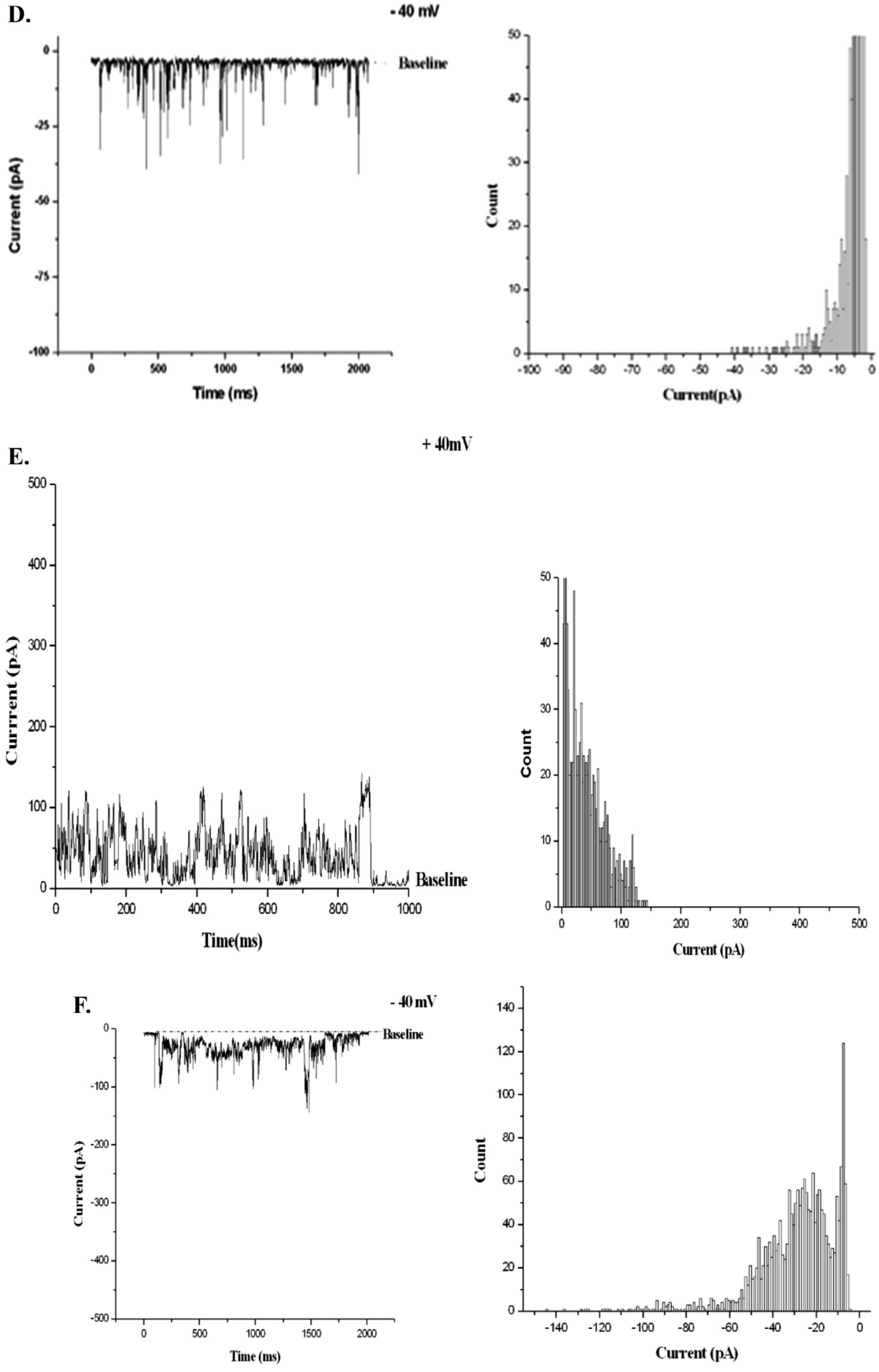

Fig. 2. (*continued*).

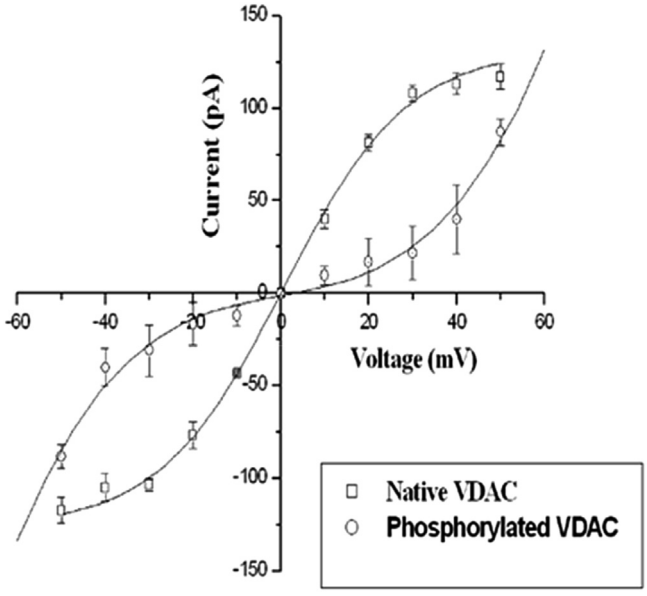

Fig. 3. Single-Channel Current–Voltage relationship (I–V plot) of full open state of Native and Phosphorylated (by JNK3) VDAC. Experimental conditions are the same as in Fig. 2. The best fit lines were drawn using Origin 5.0 software as mentioned in the Materials & Methods. Values are Mean ± S.E. of three independent set of experiments.

JNK3 is a serine–threonine kinase; phosphorylation by JNK3 would transfer negatively charged phosphate groups in place of uncharged –OH groups of serine and threonine residues. High resolution 3D structure of VDAC-1 has been reported by three groups based on the protein expressed and refolded in multiple detergent micelles or lipid bicelles from inclusion bodies in *E. coli* [23–25]. However, there is a great deal of controversy on whether the above-mentioned structure can functionally and biochemically

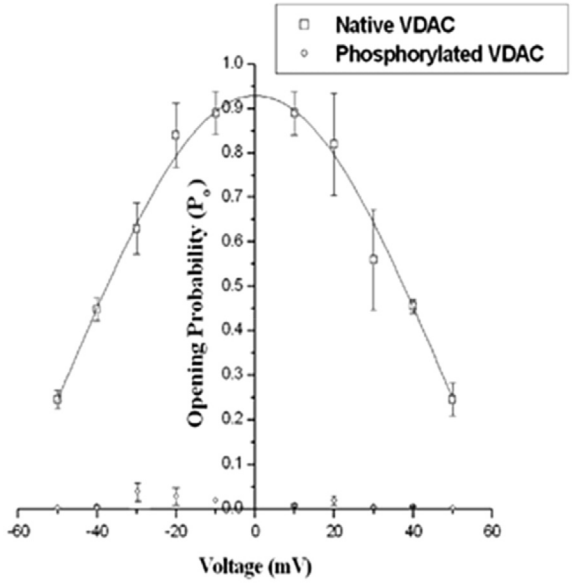

Fig. 4. Dependence of Opening Probability (P_o) of full open state of Native and Phosphorylated (by JNK3) VDAC on applied membrane potential (V). P_o versus V (mV) was calculated from Single-Channel current recordings according to the method described in Material and Methods. Experimental conditions are the same as in Fig. 2. The best fit lines were drawn using Origin 5.0 software as mentioned in the Materials & Methods. Values are Mean ± S.E. of three independent set of experiments.

mimic the VDAC's native conformation or not [26]. Given all the controversies, the trans-membrane organization of VDAC is believed, in general, to consist of a single N-terminal α-helix and either 13 or 19 trans-bilayer β-strands [26,27]. The N-terminal α-helix is believed to form the positively charged voltage sensor (predicted within 1–26 residues in VDAC1) and the trans-bilayer β barrel constitutes the positively charged pore lumen of the channel [28]. The voltage sensor is flexible and shifts between the pore lumen and the membrane surface during gating [29]. It contains two threonine and one serine residues, hence likely to undergo phosphorylation by JNK3. According to the crystal structure of mouse VDAC1, the loops which connect the β–strands of the channel, are enriched with five serine and eight threonine residues on one side. At the other side of the channel, there is one serine and four threonine sites on the loops [24]. The loops on both sides could be potential JNK3 targets. On the whole, the loops and the N-terminal voltage sensor region in VDAC have the possibility to get phosphorylated by JNK3. It may be noted that the first VDAC molecule inserts into BLM in random orientation [30]. As we have carried out VDAC phosphorylation from both the sides of the bilayer chamber all the sites are accessible to JNK3 irrespective of the orientation of the channel. However, sites accessible from the cytosolic face are only biologically relevant because they can only be accessed by JNK3 from cytosol *in vivo*. As per our view, phosphorylation of the voltage sensor would introduce negatively charged phosphate groups that would make the sensor stick to the positively charged pore lumen wall by strong electrostatic interactions, thereby partially block the mouth of the pore and hinder the ion flow leading to decrease in the single-channel current and the opening probability.

As mentioned earlier alkaline phosphatase treatment of phosphorylated VDAC reverses the channel activity, but it does not exactly reconvert it back to VDAC in its native state (Fig. 2E, F). The observed differences from the native VDAC after de-phosphorylation could be due to partial removal of the phosphate groups from the sites of phosphorylation. The partially phosphorylated VDAC is expected to have different sub-state levels and current distribution. Partial removal of phosphates might have taken place because we have used a non-specific phosphatase, i.e. alkaline phosphatase, for de-phosphorylation experiments. However, experimental verification of the above-mentioned statement has been kept pending for future work.

A significant consequence of VDAC closure due to phosphorylation could be reduction in ion, water and ATP transport from mitochondrion to cytosol. This would lead to cell death due to cytosolic ATP depletion. Further, accumulation of these substances in the mitochondrion matrix as a result of VDAC phosphorylation, can lead to swelling of the matrix, followed by rupture of the outer mitochondrial membrane and cytochrome *c* release, hence cell death [31]. It may be mentioned here that closure of VDAC by tBid protein has been reported to cause apoptosis due to similar reason [32].

We conclude that *in vitro* phosphorylation of VDAC by JNK3 leads to channel closure. This establishes our hypothesis as mentioned in the **Introduction**. Subsequently, we predict that closure of VDAC as a result of phosphorylation by JNK3 could be one of the important ways by which neurons undergo stress-induced apoptosis. The results presented here are on artificial lipid bilayer membranes although facts under *in vivo* conditions could be very different from those *in vitro*. We propose that in mitochondria-mediated apoptosis the above mentioned mechanism of JNK3 dependent apoptosis holds good and hence the overall process of neurodegeneration. Further verification of this proposed mechanism *in vivo* is difficult at this junction and is kept for our future plan.

Conflict of interest

Both the authors i.e.; Rajeev Gupta (Ph.D) and Dr. Subhendu Ghosh (Associate Professor, Dept. of Biophysics, University of Delhi South Campus, India) declare no conflict of Interest. Also, we both acknowledge Department of Atomic Energy Board of Research in Nuclear Sciences (DAE-BRNS) and Indian Council of Medical Research (ICMR), Government of India and University of Delhi for financial assistance.

Acknowledgments

We acknowledge Department of Atomic Energy, Board of Research in Nuclear Sciences (DAE-BRNS) (Grant No. 2007/37/4/BRNS/2629) and Indian Council of Medical Research (ICMR) (Grant No. 45/3/2011-BMS/CMB), Government of India and University of Delhi (Grant No. DRCH/R&D/2013-14/4155) for financial assistance.

References

[1] A.M. Distler, J. Kerner, C.L. Hoppel, Post-translational modifications of rat liver mitochondrial outer membrane proteins identified by mass spectrometry, BBA-Proteins Proteom 1774 (5) (2007) 628–636, http://dx.doi.org/10.1016/j.bbapap.2007.03.012.

[2] M.J. Shipston, Ion channel regulation by protein palmitoylation, J. Biol. Chem. 286 (11) (2011) 8709–8716, http://dx.doi.org/10.1074/jbc.R110.210005.

[3] D.J. Schulz, S. Temporal, D.M. Barry, M.L. Garcia, Mechanisms of voltage-gated ion channel regulation: from gene expression to localization, Cell. Mol. Life Sci. 65 (14) (2008) 2215–2231, http://dx.doi.org/10.1007/s00018-008-8060-z.

[4] M. Colombini, VDAC: the channel at the interface between mitochondria and the cytosol, Mol. Cell. Biochem. 256 (1–2) (2004) 107–115, http://dx.doi.org/10.1023/B:MCBI.0000009862.17396.8d.

[5] C. Mde Cesar, J.E. Wilson, All three isoforms of the voltage-dependent anion channel (VDAC1, VDAC2, and VDAC3) are present in mitochondria from bovine, rabbit, and rat brain, Arch. Biochem. Biophys. 422 (2004) 191–196, http://dx.doi.org/10.1016/j.abb.2003.12.030.

[6] J. Kerner, K. Lee, B. Tandler, C.L. Hoppel, VDAC proteomics: post-translation modifications, BBA-Biomembranes 1818 (6) (2012) 1520–1525, http://dx.doi.org/10.1016/j.bbamem.2011.11.013.

[7] C. Martel, M. Allouche, D.D. Esposti, E. Fanelli, C. Boursier, C. Henry, J. Chopineau, G. Calamita, G. Kroemer, A. Lemoine, C. Brenner, Glycogen synthase Kinase3-mediated VDAC phosphorylation controls outer mitochondrial membrane permeability during lipid accumulation, Hepatology 57 (1) (2012) 93–102, http://dx.doi.org/10.1002/hep.25967.

[8] S. Das, C. Steenbergen, E. Murphy, Does the voltage dependent anion channel modulate cardiac ischemia-reperfusion injury? Biochim. Biophys. Acta 1818 (2012) 1451–1456, http://dx.doi.org/10.1016/j.bbamem.2011.11.008.

[9] T.S. Azarashvili, I.V. Odinokova, O.V. Krestinina, Y.L. Baburina, D.E. Grachev, V.V. Teplova, E.L. Holmuhamedov, Role of phosphorylation of porin (VDAC) in regulation of mitochondrial outer membrane under normal conditions and alcohol intoxication, Biochem. Mosc. Suppl. Ser. A: Membr. Cell Biol. 5 (1) (2011) 11–20, http://dx.doi.org/10.1134/S1990747811010028.

[10] Y. Chen, M. Gaczynska, P. Osmulski, R. Polci, D.J. Riley, Phosphorylation by Nek1 regulates opening and closing of voltage dependent anion channel 1, Biochem. Biophys. Res. Commun. 394 (2010) 798–803, http://dx.doi.org/10.1016/j.bbrc.2010.03.077.

[11] A.K. Bera, S. Ghosh, Dual mode of gating of voltage-dependent anion channel as revealed by phosphorylation, J. Struct. Biol. 135 (2001) 67–72, http://dx.doi.org/10.1006/jsbi.2001.4399.

[12] J. Banerjee, S. Ghosh, Phosphorylation of rat brain mitochondrial voltage-dependent anion channel as a potential tool to control leakage of cytochrome c, J. Neurochem. 98 (2006) 670–676, http://dx.doi.org/10.1111/j.1471-4159.2006.03853.x.

[13] J. Banerjee, S. Ghosh, Bax increases the pore size of rat brain mitochondrial voltage-dependent anion channel in the presence of tBid, Biochem. Biophys. Res. Commun. 323 (2004) 310–314, http://dx.doi.org/10.1016/j.bbrc.2004.08.094.

[14] T.K. Rostovtseva, W. Tan, M. Colombini, On the role of VDAC in apoptosis: fact and fiction, J. Bioenerg. Biomembr. 37 (3) (2005) 129–142, http://dx.doi.org/10.1007/s10863-005-6566-8.

[15] V. Shoshan-Barmatz, D. Mizrachi, VDAC1: from structure to cancer therapy, Front. Oncol. 2 (2012), http://dx.doi.org/10.3389/fonc.2012.00164.

[16] J. Yu, H. Qian, Y. Li, Y. Wang, X. Zhang, X. Liang, M. Fu, C. Lin, Therapeutic effect of arsenic trioxide (As2O3) on cervical cancer in vitro and in vivo through apoptosis induction, Cancer Biol. Ther. 6 (2007) 580–586, http://dx.doi.org/10.4161/cbt.6.4.3887.

[17] E.T. Coffey, Nuclear and cytosolic JNK signalling in neurons, Nat. Rev. Neurosci. 15 (5) (2014) 285–299, http://dx.doi.org/10.1038/nrn3729.

[18] R.J. Davis, Signal transduction by the JNK group of MAP kinases, in: Inflammatory Processes, Birkhäuser Basel, 2000, pp. 13–21, http://dx.doi.org/10.1016/S0092-8674(00)00116-1.

[19] S. Eminel, A. Klettner, L. Roemer, T. Herdegen, V. Waetzig, JNK2 translocates to the mitochondria and mediates cytochrome c release in PC12 cells in response to 6-hydroxydopamine, J. Biol. Chem. 279 (2004) 55385–55392, http://dx.doi.org/10.1074/jbc.M405858200.

[20] Y. Zhao, T. Herdegen, Cerebral ischemia provokes a profound exchange of activated JNK isoforms in brain mitochondria, Mol. Cell. Neurosci. 41 (2009) 186–195, http://dx.doi.org/10.1016/j.mcn.2009.02.012.

[21] A. Mahfoudh-Boussaid, M.A. Zaouali, T. Hauet, K. Hadj-Ayed, A.H. Miled, S. Ghoul-Mazgar, D. Saidane-Mosbahi, J. Rosello-Catafau, H.B. Abdennebi, Attenuation of endoplasmic reticulum stress and mitochondrial injury in kidney with ischemic post-conditioning application and trimetazidine treatment, J. Biomed. Sci. 19 (1) (2012) 1–14, http://dx.doi.org/10.1186/1423-0127-19-71.

[22] V. de Pinto, G. Prezioso, F. Palmieri, A simple and rapid method for the purification of the mitochondrial porin from mammalian tissues, BBA-Biomembranes 905 (2) (1987) 499–502.

[23] S. Hiller, R.G. Garces, T.J. Malia, V.Y. Orekhov, M. Colombini, G. Wagner, Solution structure of the integral human membrane protein VDAC-1 in detergent micelles, Science 321 (5893) (2008) 1206–1210, http://dx.doi.org/10.1126/science.1161302.

[24] R. Ujwal, D. Cascio, J.P. Colletier, S. Faham, J. Zhang, L. Toro, P. Ping, J. Abramson, The crystal structure of mouse VDAC1 at 2.3 A resolution reveals mechanistic insights into metabolite gating, Proc. Natl. Acad. Sci. U. S. A. 105 (2008) 17742–17747, http://dx.doi.org/10.1073/pnas.0809634105.

[25] M. Bayrhuber, T. Meins, M. Habeck, S. Becker, K. Giller, S. Villinger, C. Vonrhein, C. Griesinger, M. Zweckstetter, K. Zeth, Structure of the human voltage-dependent anion channel, Proc. Natl. Acad. Sci. U. S. A. 105 (40) (2008) 15370–15375, http://dx.doi.org/10.1073/pnas.0808115105.

[26] M. Colombini, The published 3D structure of the VDAC channel: native or not? Trends Biochem. Sci. 34 (8) (2009) 382–389, http://dx.doi.org/10.1016/j.tibs.2009.05.001.

[27] S. Hiller, J. Abramson, C. Mannella, G. Wagner, K. Zeth, The 3D structures of VDAC represent a native conformation, Trends Biochem. Sci. 35 (2010) 514–521, http://dx.doi.org/10.1016/j.tibs.2010.03.005.

[28] L. Thomas, E. Blachly-Dyson, M. Colombini, M. Forte, Mapping of residues forming the voltage sensor of the voltage-dependent anion-selective channel, Proc. Natl. Acad. Sci. U. S. A. 90 (1993) 5446–5449.

[29] J. Song, C. Midson, E. Blachly-Dyson, M. Forte, M. Colombini, The sensor regions of VDAC are translocated from within the membrane to the surface during the gating processes, Biophys. J. 74 (1998) 2926–2944, http://dx.doi.org/10.1016/S0006-3495(98)78000-2.

[30] E.J. Marques, C.M. Carneiro, A.S. Silva, O.V. Krasilnikov, Does VDAC insert into membranes in random orientation? Biochim. Biophys. Acta 1661 (1) (2004) 68–77, http://dx.doi.org/10.1016/j.bbamem.2003.11.018.

[31] Matthew G. Vander Heiden, Navdeep S. Chandel, Xiao Xian Li, Paul T. Schumacker, Marco Colombini, Craig B. Thompson, Outer mitochondrial membrane permeability can regulate coupled respiration and cell survival, Proc. Natl. Acad. Sci. 97 (9) (2000) 4666–4671, http://dx.doi.org/10.1073/pnas.090082297.

[32] T.K. Rostovtseva, B. Antonsson, M. Suzuki, R.J. Youle, M. Colombini, S.M. Bezrukov, Bid, but not Bax, regulates VDAC channels, J. Biol. Chem. 279 (2004) 13575–13583, http://dx.doi.org/10.1074/jbc.M310593200.